J. Physiol. (1985), **368**, *pp.* 213–226
With 5 text-figures
Printed in Great Britain

TIGHTNESS OF THE BLOOD–BRAIN BARRIER AND EVIDENCE FOR BRAIN INTERSTITIAL FLUID FLOW IN THE CUTTLEFISH, *SEPIA OFFICINALIS*

BY N. JOAN ABBOTT*, MAGNUS BUNDGAARD† AND HELEN F. CSERR‡

*From the * Department of Physiology, King's College, Strand, London WC2R 2LS, † Institute of Medical Physiology A, University of Copenhagen, Blegdamsvej 3, DK-2200 Copenhagen N, Denmark, and the ‡ Section of Physiology and Biophysics, Brown University, Providence, RI 02912, U.S.A.*

(*Received 27 November 1984*)

SUMMARY

1. Cephalopod molluscs have complex brains and behaviour, yet little is known about the permeability of their blood–brain interface. The accompanying paper characterized the fluid compartments of the brain and presented evidence for restricted permeability of the blood–brain interface to albumin. The present paper investigates the permeability of the interface to small non-electrolytes.

2. [^{14}C]Polyethylene glycol (PEG, mol. wt. 4000), and [^{51}Cr]EDTA (mol. wt. 342) were injected intravenously or intramuscularly, and their penetration into brain and muscle studied up to 48 h. Tracers equilibrated with muscle interstitial fluid (ISF) at relatively short times, but in brain ISF reached only 0·5–0·65 × their plasma concentration. This is qualitative evidence for the presence in brain of a barrier to these molecules and an efficient drainage mechanism for ISF.

3. Quantitative treatment of the uptake data allows calculation of the permeability × surface area product (*PS*) and the permeability coefficient (*P*). For the brain *PS* and *P* are in the range $1–3 \times 10^{-4}$ ml g^{-1} min^{-1} and $1–3 \times 10^{-8}$ cm s^{-1} respectively, (PEG), and 3×10^{-4} ml g^{-1} min^{-1} and $3–4 \times 10^{-8}$ cm s^{-1} respectively (Cr-EDTA). The *P* values are close to those reported for mammalian brain.

4. Assuming that the lack of equilibration in brain is due to ISF flow, the rate of flow can be calculated. Values for vertical and optic lobe are approximately 0·2 μl g^{-1} min^{-1}, again close to those reported for mammalian brain.

5. It is concluded that the tightness of the *Sepia* blood–brain barrier approaches that of mammals, and a flowing ISF system is present. An association between a tight barrier and higher central nervous system integrative function is suggested. The significance of these findings for the evolution of control of the brain microenvironment is discussed.

Experiments were carried out at: The Marine Biological Association Laboratory, Citadel Hill, Plymouth PL1 2PB.

INTRODUCTION

The accompanying paper presented information on the ionic content, extracellular space and vascular volume of *Sepia* brain and muscle, together with evidence that the blood–brain interface in this species is relatively impermeable to protein (Abbott, Bundgaard & Cserr, 1985). In the present paper we investigate the permeability of the blood–brain barrier to small non-electrolytes, polyethylene glycol (PEG) and Cr-EDTA. A quantitative treatment allows us to estimate the permeability × surface area product (*PS*) for small solutes, and by the use of separately determined estimates of blood vessel surface area (*S*), to derive the permeability coefficient (*P*), the first time this has been possible for any invertebrate blood–brain barrier. This permits comparison of the blood–brain barrier permeability in *Sepia* with that of vertebrates. We present evidence that the tightness of the blood–brain barrier in *Sepia* approaches that of mammals.

Since vertebrate brain is formed embryologically from the neural tube, adult brain retains a central fluid-filled cavity, the cerebral ventricular system, albeit severely reduced in some groups (e.g. hagfish, Agnatha). The ventricles contain cerebrospinal fluid (CSF), secreted continuously by choroid plexuses and draining back into the venous system by various routes, predominantly via the arachnoid villi in mammals. The interstitial fluid (ISF) of brain is in free communication with the CSF across most of the ependymal lining of the ventricles (reviewed by Bradbury, 1979).

An additional 'extra-choroidal' source of CSF/ISF has been proposed; in experiments designed to eliminate choroid plexus fluid secretion (e.g. removal of plexus, or perfusion of the 'aqueduct' between 3rd and 4th ventricles, a part of the system without a choroid plexus), fluid production is still observed, at rates accounting for up to 30% of the normal CSF (reviewed by Cserr, 1971).

The source of this 'extra-choroidal' fluid is uncertain, but could be the brain parenchymal vessels themselves. Recently, evidence for ISF production and outflow has been obtained in mammalian brain (Cserr & Ostrach, 1974; Cserr, Cooper & Milhorat, 1977; Rosenberg, Kyner & Estrada, 1980). Radioactive extracellular tracers of different molecular weights injected into brain parenchyma are cleared from brain at comparable rates, suggesting that bulk fluid flow rather than simple diffusion is responsible (Cserr, Cooper, Suri & Patlak, 1981; Szentistvanyi, Patlak, Ellis & Cserr, 1984). Since substances injected at certain sites in the brain interstitium (such as caudate nucleus) appear eventually in cervical lymph without reaching high levels in bulk (cisternal) CSF, it appears that the ISF and CSF systems may be relatively independent in some parts of vertebrate brain (Bradbury, Cserr & Westrop, 1981; Szentistvanyi *et al.* 1984).

Cephalopod molluscs have no cerebral ventricles or CSF, and therefore offer an opportunity for investigating the presence of ISF production and flow in a central nervous system without the complications of a ventricular compartment or CSF production. We present evidence consistent with continuous turnover of cerebral ISF in *Sepia*, and suggest that a flowing brain ISF may be found in all animals with a relatively tight blood–brain barrier. A preliminary account of this work has been published (Abbott, Bundgaard & Cserr, 1982).

METHODS

Animals, anaesthesia and operative technique were as in the previous paper (Abbott *et al.* 1985).

Isotopic tracer studies

The permeability of the blood–brain interface was estimated with [^{51}Cr]EDTA (Radiochemical Centre, Amersham, England), and [^{14}C]PEG, mol. wt. 4000 (New England Nuclear, Boston, MA, USA or Radiochemical Centre, Amersham, England). Isotope was injected intravenously or intramuscularly (see below) and tissues and fluids sampled and assayed for radioactivity as previously described (Abbott *et al.* 1985). Doses were 5–8 μCi/100 g for EDTA and 1–5 μCi/100 g for PEG. Knowledge of the concentration of tracer in the tissue parenchyma (brain or muscle) at a given time, together with the plasma concentration profile for the tracer up to that time, permits calculation of the *PS* product of the blood–tissue interface and the rate of ISF flow (see Theory, below).

[^{14}C]-PEG. In the first series of experiments (PEG series A, 2–3 h), animals were anaesthetized with 0·2 % chloral hydrate, and [^{14}C]PEG was injected as a single bolus into the caudal end of the anterior vena cava over 5–10 s. The animals were allowed to recover in flowing sea-water tanks, being re-anaesthetized as necessary for taking blood samples. Six to eight blood samples were taken from the rostral portion of the anterior vena cava at increasing intervals over the 2 or 3 h experimental period before the final blood sample and sacrifice of the animal.

In the second series of experiments (PEG series B, 3–48 h), tracer was injected intravenously, plasma samples taken at intervals, and tissue activity measured after either 3, 6, 24, or 48 h.

[^{51}Cr]EDTA. EDTA was injected into mantle muscle at multiple sites approximately 1 cm lateral to the stellate ganglion. All animals received an injection at zero time; in 24 h experiments, a second injection was given at 12 h. Plasma was sampled as for PEG series B and tissue activity was measured after either 6 or 24 h.

Assay of radiochemical purity of [^{14}C]PEG. The radiopurity of stock isotope solution, of *Sepia* plasma, and of buffer extracts of brain was assayed by gel filtration on Sephadex G-75 as described previously (Cserr *et al.* 1981).

Morphometric analysis of blood vessels

A parallel morphometric study of the blood–tissue interface was undertaken (Abbott & Bundgaard, 1985). Briefly, *Sepia* brain and muscle were fixed by aortic perfusion with 2·5 % glutaraldehyde and 2 % formaldehyde in 0·1 M-Na cacodylate buffer with NaCl 24 g l^{-1}, post-fixed in OsO_4, and after dehydration, embedded in Epon. 1 μm sections were photographed at standard magnification ($\times$ 234) and blood vessel profiles traced onto transparent overlays. For calculation of surface area of the blood–tissue exchange interface, a grid of 288 uniform short lines, total length 142·2 cm, was superimposed on the tracings. Surface area density S_v was calculated from the standard morphometric relationship (Weibel, 1979):

$$S_v = 2\Sigma I_c / \Sigma L_{total} \text{ cm}^{-1}, \quad (1)$$

where ΣI_c is the total number of intercepts of the grid lines with the walls of microvessels, and ΣLtotal is the total length of grid line superimposed on the tracing, corrected for magnification. Since most small vessels in *Sepia* have diameters in the range 2–15 μm, 20 μm was considered a suitable cut-off point for the analysis. We have accordingly defined 'microvessels' as those with diameters less than 20 μm.

Theory

The results for [^{14}C]PEG and [^{51}Cr]EDTA were analysed according to a two compartment model of plasma–tissue exchange. The model assumes, (1) that tracer distributes passively across the capillary wall, (2) that tracer is cleared from the tissue by bulk flow of ISF and, (3) that tracer within the tissue remains confined to the extracellular space.

Following systemic administration of tracer, the uptake of tracer into the tissue is given by:

$$dA_e/dt = K_i C_p - k_0 A_e, \quad (2)$$

where A_e is the amount of tracer in the tissue parenchyma per unit mass of tissue (d.p.m. g^{-1}),

K_1 is the blood-to-tissue transfer constant (ml g^{-1} min^{-1}), C_p is the concentration of tracer in plasma (d.p.m. ml^{-1}) and k_0 is the tissue-to-blood transfer constant (min^{-1}).

K_1 is dependent on both permeability and blood flow. When $PS \ll$ blood flow, a condition that is satisfied by substances used in this study, transfer of tracer into the tissue is independent of tissue blood flow (Fenstermacher, Blasberg & Patlak, 1981) and

$$K_1 \simeq PS, \tag{3}$$

where P is the permeability coefficient of a test substance per cm^2 of capillary surface (cm min^{-1}) and S is capillary surface area per gram of tissue (cm^2 g^{-1}).

Given that tracer efflux from the tissue has two components, diffusion into capillary plasma and bulk flow, it follows that

$$k_0 = PS/V_e + K_f/V_e, \tag{4}$$

where V_e is the volume of ISF (ml g^{-1}) and K_f is the rate constant for ISF flow (ml g^{-1} min^{-1}). The transfer constant for total efflux, k_0, has different units from PS and K_f. To express PS and K_f in units comparable to k_0 these terms are divided by V_e.

For [^{14}C]PEG, following intravenous injection at $t = 0$, the tracer concentration in plasma declines gradually by loss into extravascular spaces. This decline can be approximated by a multi-exponential equation:

$$C_p = B_1 e^{-k_1 t} + B_2 e^{-k_2 t} + B_3 e^{-k_3 t} \tag{5}$$

in which the ks are rate constants, the Bs are coefficients and t is time. Combining eqns (2), (3) and (5) and solving, gives A_e at any time as a function of PS and k_0

$$A_e = PS \sum_{n=1}^{3} \frac{B_n}{k_0 - k_n} (e^{-k_n t} - e^{-k_0 t}). \tag{6}$$

At early times (3 h or less), backflux of PEG from tissue to blood is much less than influx into the tissue and can be ignored. Under this condition, combining eqns. (2) and (3) yields

$$dA_e/dt = PS C_p. \tag{7}$$

Eqn. (7) is integrated to give the following expression, when $A_e = 0$ at $t = 0$:

$$PS \simeq \frac{A_e}{\int_0^t C_p \, dt}. \tag{8}$$

Eqn. (8) is similar to the one developed by Ohno, Pettigrew & Rapoport (1978).

For [^{51}Cr]EDTA, plasma concentration C_p is maintained nearly constant by slow release from an intramuscular injection. Combining eqns. (2) and (3) and solving for PS when C_p is constant yields

$$PS = \frac{k_0 A_e}{C_p(1 - e^{-k_0 t})}. \tag{9}$$

Inspection of eqns. (6), (8) and (9) reveals that the determination of PS is independent of the value assumed for tissue ISF volume. In contrast, determination of K_f is dependent on this parameter, as shown in eqn. (4).

Calculation of A_e and A_e/V_e

In order to calculate PS and k_0 from the experimental results, the amount of isotope measured in the tissue A_m (d.p.m. g^{-1}) must be corrected for that part contained in the blood vessels. The amount of isotope in the parenchyma (i.e. extravascular tracer), A_e, was calculated from:

$$A_e = A_m - V_v C_p, \tag{10}$$

where V_v is the vascular volume (ml g^{-1}) and C_p is the concentration of tracer in the terminal plasma sample (d.p.m. ml^{-1}). Values for V_v, from the previous paper (Abbott *et al.* 1985), were taken as 0·034 for vertical lobe, 0·056 for optic lobe, 0·022 for valve muscle and 0·004 for tentacle muscle.

The volume of ISF, V_e (ml g^{-1}), was estimated from:

$$V_e = 0{\cdot}76 \times \text{Cl space} - V_v \tag{11}$$

using values for Cl space and V_v from the previous paper (Abbott *et al.* 1985). Estimated values for V_e were 0·168 for vertical lobe, 0·118 for optic lobe, 0·256 for valve muscle and 0·177 for tentacle muscle.

Tracer concentration in tissue ISF, Figs 2, 3 and 4, was obtained by dividing the amount of tracer in the parenchyma, A_e, by ISF volume, V_e.

RESULTS

Radioisotopic tracer studies

Radiochemical purity of [^{14}C]*PEG.* The radiochemical purity of PEG was assayed by gel filtration. Most of the radioactivity in pooled samples of plasma and of brain from *Sepia* killed either 3 or 6 h after isotope injection chromatographed as a single peak with the same mobility as radioactivity from the stock injection solution. There was also a small second peak of radioactivity in the brain with a higher molecular weight than PEG. The amount of this component was small (approximately 6 % of total tissue radioactivity, in both the 3 h and 6 h brain samples).

Tracer blood activity curves. Estimation of penetration of isotopes into tissue was made following intravascular ([^{14}C]PEG) or intramuscular ([^{51}Cr]EDTA) injection. Interpretation of these experiments requires a knowledge of the activity of isotope in plasma during the experimental period. For [^{14}C]PEG series A, plasma activity curves were determined in each animal. In series B, a composite curve was produced by pooling results from several animals (Fig. 1*A*). PEG was initially cleared rapidly from blood, but by 6 h plasma activity was falling more slowly. To avoid rapid clearance of the smaller molecule [^{51}Cr]EDTA from blood, it was injected intramuscularly, an injection site within the mantle muscle being deliberately chosen in a poorly perfused part, so that the injection site would act as a slow release depot of isotope. The relatively stable plasma concentration of isotope over 24 h (Fig. 1*B*) confirms the effectiveness of this method.

Failure of PEG and EDTA to reach equilibrium in brain

The concentration of tracer in ISF within each tissue at the end of the experiment was calculated as outlined in Methods. The ISF concentration as a fraction of plasma concentration is plotted in Fig. 2 for [^{14}C]PEG (series B) and in Fig. 3 for [^{51}Cr]EDTA. Steady-state tracer concentration in ISF of *Sepia* brain is consistently much less than that of plasma, approximately 0·5 × that of plasma at 48 h for PEG and 0·65 × that of plasma at 24 h for EDTA, whereas near equilibrium has occurred between ISF and plasma in muscle. The simplest explanation for the failure of PEG and EDTA to reach equilibrium in brain is that ISF containing the tracer in low concentration is continuously being formed and draining out of brain.

Fig. 4 presents values for ISF concentration of PEG (d.p.m. ml^{-1}) at each time in series B for comparison with best fit lines obtained by modelling the results (see below).

Determination of PS

In the short term PEG experiments (series A, 2–3 h), *PS* was calculated individually for each animal from the tissue concentration and the integral of the plasma concentration during the course of the experiment according to eqn. (8). This

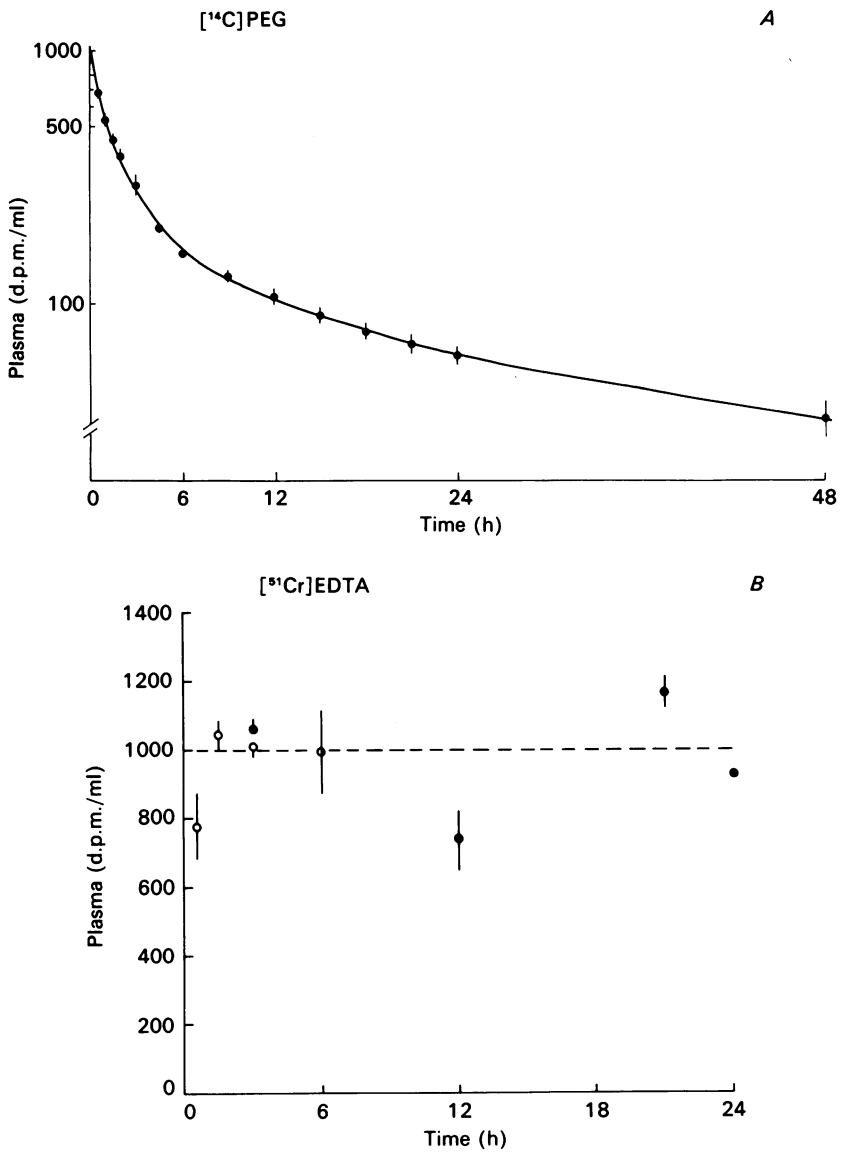

Fig. 1. Plasma activity curves for, *A*, [^{14}C]PEG, series B and, *B*, [^{51}Cr]EDTA. In *A*, $C_p = 666\,e^{-0.014t} + 227\,e^{-3.21 \times 10^{-3} t} + 107\,e^{-3.85 \times 10^{-4} t}$. Pooled data from twelve animals normalized to activity at 6 h (= 100) and then scaled up so activity at zero time = 1000 d.p.m./ml. In *B*, data normalized so that activity at 6 h = 1000 d.p.m./ml. Open circles: 6 h experiments. Filled circles: 24 h experiments. n = 3–5 animals per point.

equation assumes negligible backflux of tracer from the tissue. There was no significant difference between *PS* derived from 2 h (n = 7) and 3 h (n = 2) experiments. The results have therefore been pooled, and the mean of all nine experiments used for further calculations (Table 1).

In the second series of PEG experiments (series B, 3–48 h), *PS* was calculated

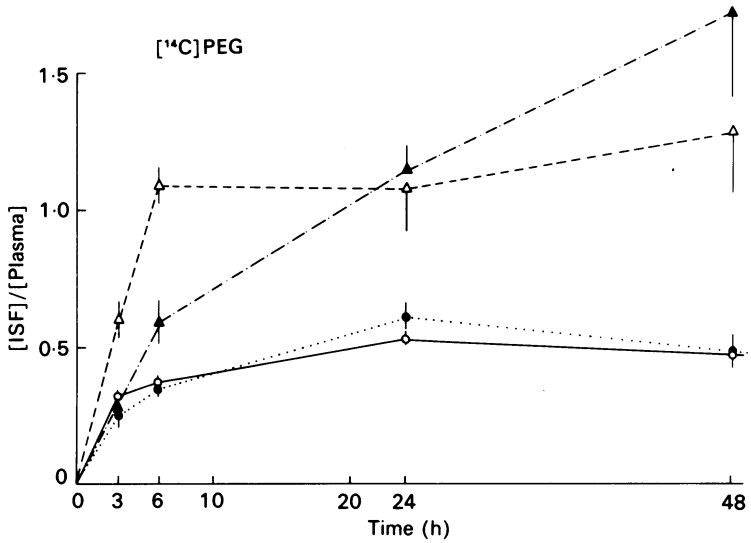

Fig. 2. [^{14}C]PEG concentration in tissue ISF as a fraction of plasma concentration at each time, series B. Vertical lobe: open circles and continuous line. Optic lobe: filled circles and dotted line. Valve muscle: open triangles and dashed line. Tentacle muscle: filled triangles and dots and dashes.

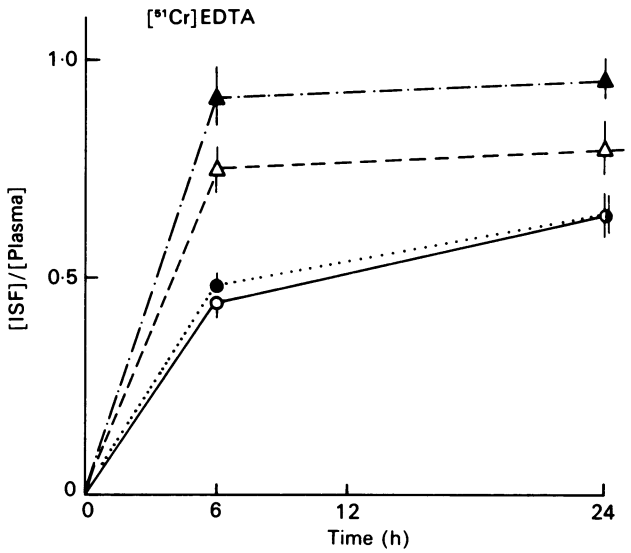

Fig. 3. [^{51}Cr]EDTA concentration in tissue ISF as a fraction of plasma concentration. Symbols as in Fig. 2.

according to eqn. (6). This equation allows for tracer backflux from the tissue. Fewer blood samples were taken in these experiments and the results were analysed using the 'composite' plasma curve of Fig. 1*A*. This curve can be approximated by the sum of three exponentials, eqn. (5), with the constants given in the legend to Fig. 1. The parameters of eqn. (6), PS and k_0, were estimated by means of a

non-linear least squares fit and best fit lines derived using these values of PS and k_0 are shown in Fig. 4. PS values for these experiments (PEG series B) are of the same order as those for the short term experiments (series A) (Table 1).

PS for [^{51}Cr]EDTA (6 or 24 h experiments) was calculated using eqn. (9) on the assumption of a constant plasma concentration of test substance. This equation also allows for tracer efflux from the tissue. An iterative method was used to derive PS and k_0. As anticipated on the basis of molecular size, PS is greater for EDTA than for the larger PEG tracer (Table 1).

Determination of K_f

K_f was calculated according to eqn. (4) using values for PS and k_0 derived from the tracer experiments (above) and values for V_e estimated on the basis of results from the previous paper (Abbott *et al.* 1985), as outlined in the Methods. Rates of ISF drainage from brain tissue, K_f, calculated independently for the PEG and EDTA results were closely similar (Table 1).

Since K_f is dependent on V_e it is appropriate to consider the effect of an error in the estimation of V_e on the results. Taking PEG results for the optic lobe as an example, it can be shown that a 20% error in V_e would lead to a change of 30% (0·05 μl g^{-1} min^{-1}) in the value for bulk flow (0·15 μl g^{-1} min^{-1}). In order to obtain zero bulk flow, the true value of V_e would have to be 61% less than predicted (0·046 ml g^{-1} as opposed to the estimated value of 0·118 ml g^{-1}). In the previous paper it was shown that the brain extracellular space as estimated from Cl space (the basis for V_e used here) was in good agreement with the steady-state distribution space of [^{51}Cr]EDTA in isolated tissues incubated *in vitro*, in which the blood–brain barrier was by-passed (Abbott *et al.* 1985). Large errors in the estimate of interstitial space, of the magnitude required to negate the conclusion that there is bulk flow of interstitial fluid, are therefore unlikely.

Morphometric analysis of blood vessels

Surface area density for exchange microvessels of brain vertical and optic lobe, S_v, was calculated as $134 \pm 8{\cdot}8$ and $176 \pm 9{\cdot}5$ cm^{-1} respectively (Abbott & Bundgaard, 1985). For valve and tentacle muscle, values could not be determined with the same accuracy (because of the smaller sample number), but S_v was estimated as 68 ± 4 and 14 cm^{-1} respectively.

Calculation of permeability coefficient P

The estimate of the surface area for exchange, S, derived from the morphometric analysis, permits calculation of P from PS determined for PEG and EDTA. The results are given in Table 1, with values for mammalian brain and muscle for comparison.

DISCUSSION

Comparison of the blood–brain barrier in Sepia and in mammals

Classical studies of the vertebrate blood–brain barrier have used inulin and sucrose as probe molecules and limited penetration into brain in comparison with muscle is used as a qualitative indication of the presence of a blood–brain barrier (Bradbury,

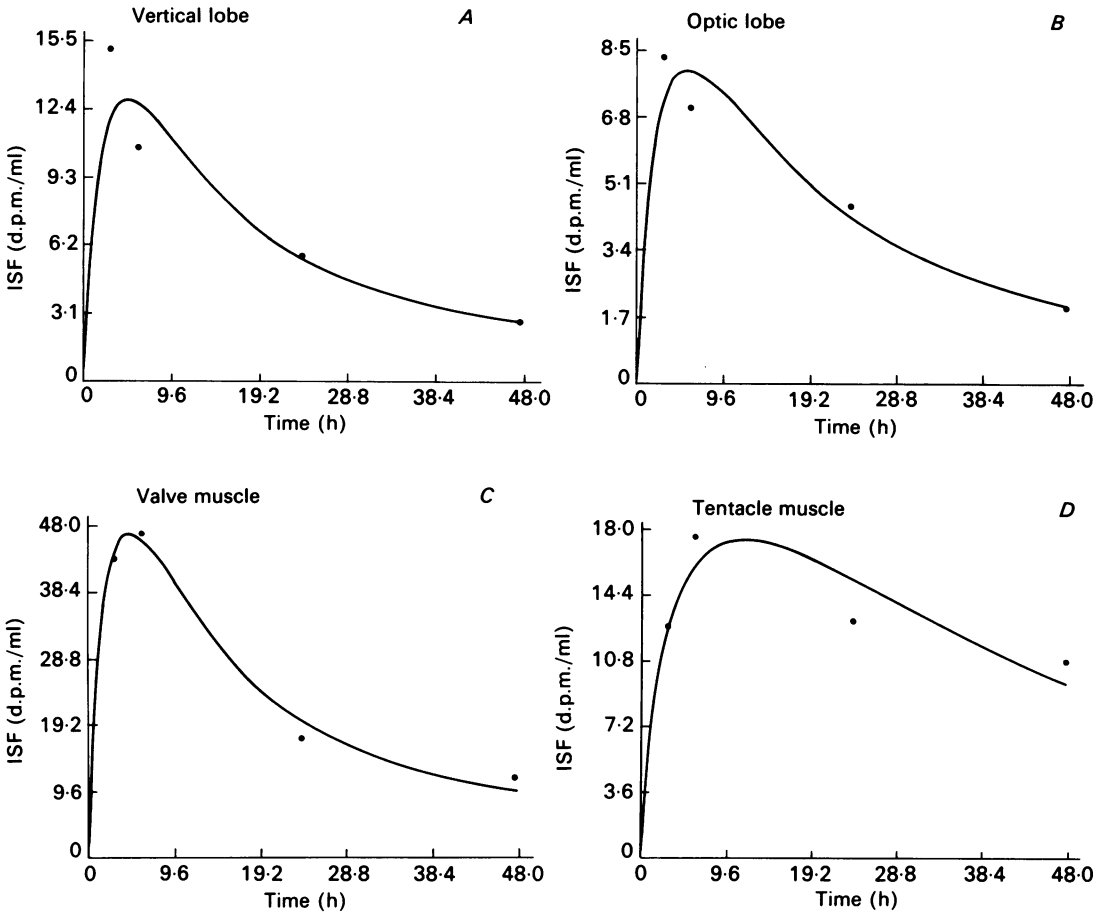

Fig. 4. [^{14}C]PEG concentration in tissue ISF, series B. *A*, vertical lobe, *B*, optic lobe, *C*, valve muscle, *D*, tentacle muscle. Filled circles are experimental results. Lines are best fit lines drawn according to eqn. (6), using the values of *PS* given in Table 1.

1979). In the present studies, [^{14}C]PEG was chosen for its similarity in size to inulin (*ca.* 25 Å mol. diameter), and [^{51}Cr]EDTA for its similarity to sucrose (*ca.* 10 Å mol. diameter). However, PEG and EDTA have advantages over inulin and sucrose as extracellular tracers since they are less subject to cellular uptake and breakdown (Schmidt-Nielsen, Renfro & Benos, 1972; Schmidt-Nielsen & Renfro, 1975; Poole-Wilson & Cameron, 1975). The more restricted penetration of tracers into brain compared with muscle in *Sepia* (Figs. 2 and 3) indicates that this species also has an effective blood–brain barrier.

The results of our quantitative analyses (Table 1) show that for both PEG and EDTA, the permeability (*P*) of the *Sepia* blood–brain barrier is low, and similar to that of mammals. *Sepia* muscle vessels are at least an order of magnitude more permeable; for EDTA for example, tentacle muscle permeability is about sixty-eight times greater than brain optic lobe permeability. These results therefore show clearly that cerebral and muscle blood vessels in *Sepia* are quantitatively different in

TABLE 1. Permeability × surface area product PS (ml g^{-1} min^{-1} × 10^4), permeability P (cm s^{-1} × 10^8) and rate of ISF flow K_f (μl g^{-1} min^{-1}) for *Sepia* tissues calculated for PEG and EDTA. Values for mammal (rat) are included for comparison, assuming inulin behaves like PEG, and sucrose like EDTA.

Animal	Test molecule	Brain		Muscle	
		v.l.	o.l.	v.m.	t.m.
	PEG: Series A				
Sepia	*PS*	2·6±0·38	2·4±0·11	7·6±0·53	2·8±0·41
	P	3·2±0·47	2·3±0·32	20	31
	Series B				
	PS	1·7±0·39	1·0±0·14	6·4±1·05	1·5±0·20
	K_f	0·27	0·15	~0	~0
	P	2·1±0·49	0·9±0·13	16	17
Mammal	*P*	0·25–2·5[1,4,5]		200[2]	
	K_f	0·11–0·29[3]			
	EDTA				
Sepia	*PS*	3·5	2·9	17	16
	K_f	0·19	0·17	~0	~0
	P	4·3	2·8	44	180
Mammal	*P*	0·7–7[1,4,5]		1020[2]	

V.l., vertical lobe; o.l., optic lobe; v.m., valve muscle; t.m., tentacle muscle.
References: [1] Bradbury (1979); [2] Paaske (1980); [3] Szentistvanyi *et al.* (1984); [4] Ohno *et al.* (1978); [5] Amtorp (1980).

permeability, and they provide clear evidence for the effectiveness of the blood–brain barrier in a cephalopod mollusc. This study is the first in which it has been possible to compare an invertebrate barrier with that of vertebrates in a quantitative way.

Failure of PEG and EDTA to equilibrate with brain ISF: evidence for a flow of ISF

Steady-state tracer concentration in ISF is consistently much less than that of plasma, with ISF/plasma ratios being approximately 0·50 (PEG) and 0·65 (EDTA) in both vertical and optic lobes, compared with near 1·0 in muscle. This is strikingly reminiscent of the findings in vertebrate brain, where extracellular tracers such as sucrose and inulin reach an interstitial concentration in the steady state equivalent to 0·14–0·23 × the plasma concentration (calculated from figures in Bradbury (1979) assuming the ISF accounts for 21 % of brain volume (Nicholson & Phillips, 1981)). Failure of extracellular tracers to equilibrate with ISF, despite a finite permeability of the blood–brain barrier to these tracers, implies the presence of an effective excretory mechanism for clearing substances from the interstitium.

The classical explanation for the relatively low concentration of extracellular tracers in vertebrate brain ISF has been that substances are cleared from the interstitium by net diffusion, from brain to CSF (Davson, Kleeman & Levin, 1963). This explanation, known as the 'sink' hypothesis, is based on evidence that many polar compounds are found in much lower concentration in CSF than in ISF. According to this hypothesis, net transport from brain ISF to CSF via diffusion is

equal in the steady state to net transport (mainly by bulk drainage) from CSF to blood. This mechanism depends on the continuous production and drainage of CSF and on a limited permeability of the choroid plexus to maintain steady-state concentration gradients between ISF and CSF. Clearly, an alternative mechanism is required to explain the failure of PEG and EDTA to equilibrate with ISF in *Sepia* brain, as cephalopods lack a CSF system.

Bulk flow of ISF has also been suggested as a mechanism for clearing substances from brain (e.g. Cserr, 1971). Recent studies have shown that bulk drainage of ISF into the lymphatics (e.g. associated with the olfactory nerves in the nose) by a route not involving the bulk cisternal CSF compartment, contributes to the removal of protein from the mammalian brain (Bradbury *et al.* 1981; Szentistvanyi *et al.* 1984). This same mechanism may also explain the observation that equilibrium of tracers between plasma and brain ISF is not achieved in the hagfish, a species with no choroid plexus and only a rudimentary CSF/ventricular system (at steady state, PEG ISF concentration is approximately 0·3–0·35 × that of plasma (Bundgaard & Cserr, 1981)). A model illustrating this hypothesis is shown in Fig. 5.

If the *Sepia* results are also due to bulk flow of ISF out of brain, the rate of flow K_f can be calculated from eqn. (4) as discussed above. The PEG data are compatible

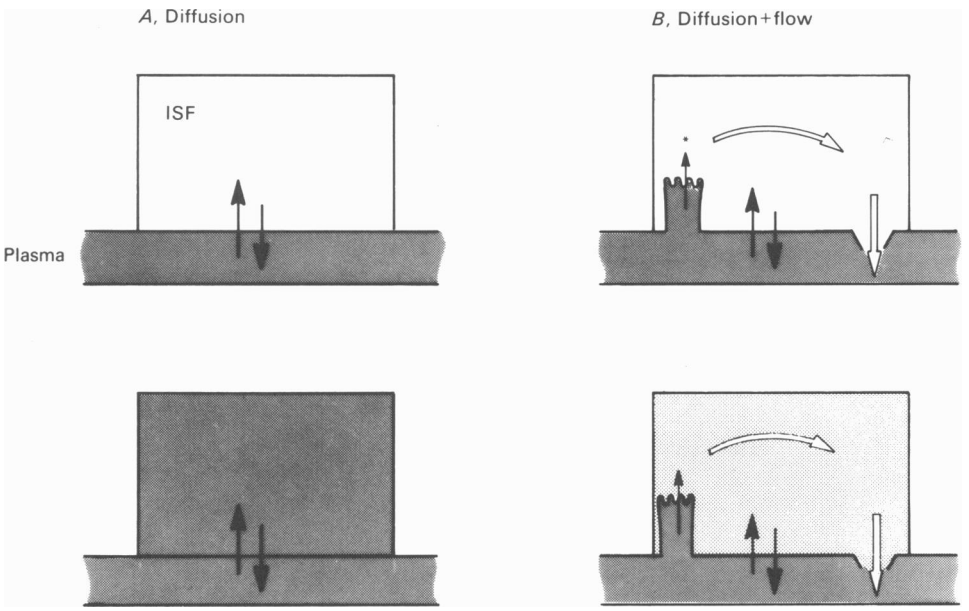

Fig. 5. Model illustrating the effects of bulk ISF flow on extracellular tracer distribution, initially (above) and at $t = \infty$ (below). Tracer concentration is indicated by stippling. In *A*, exchange across the blood vessel wall is assumed to occur only by diffusion (large black arrows); at $t = \infty$, tracer concentration in ISF (C_{ISF}) is equal to plasma concentration (C_{PL}). In *B*, ISF is being continuously produced (e.g. as a secretion, small arrow), but the new fluid contains the tracer in low concentration because of the limited permeability of the blood–brain barrier. Bulk flow of ISF (open arrows) removes tracer continuously, back into blood, so that at $t = \infty$, $C_{ISF} < C_{PL}$.

with a flow of ISF in vertical lobe of 0·27 and in optic lobe of 0·15 μl g^{-1} min^{-1}. Comparable figures for the flow of ISF in mammals are 0·11–0·29 μl g^{-1} min^{-1} (Szentistvanyi *et al.* 1984).

Values for K_f calculated from the EDTA results, given in Table 1, are close to those calculated from the PEG results, further evidence that bulk flow of fluid out of brain is a reasonable explanation for the failure to reach equilibrium.

Alternative explanations for the lack of equilibration need to be considered. One possibility is that the true extracellular space is smaller than estimated, and that the extracellular tracers equilibrate fully with this space. However, the correspondence between extracellular space estimated from Cl space, and from [^{51}Cr]EDTA *in vitro* (see above) makes this unlikely.

Lack of equilibration could also conceivably be due to steric exclusion by an extracellular matrix (Comper & Laurent, 1978), the exclusion being a function of tracer molecular size. However, the apparent lack of exclusion in tissues incubated *in vitro* would then need to be explained. Applying the equation $K_{av} = \exp(-L\pi(r_s - r_r)^2)$ where K_{av} is the volume fraction available to the tracer, L is the length of matrix fibre rods per unit volume, and r_s and r_r the radii of tracer molecule and matrix rods respectively, the *Sepia* results would require an extracellular matrix with fibres of 2·2 nm radius. This is at least six times greater than the radius of the polysaccharides that make up the bulk of the extracellular matrix in connective tissues and brain of invertebrates and vertebrates (hyaluronic acid and chondroitin sulphate; Ashhurst & Costin, 1971; Margolis & Margolis, 1979). Steric exclusion is therefore an unlikely explanation for our results.

Although the ISF is shown originating at a particular site in Fig. 5 (marked *), no specialized secretory tissue equivalent to the choroid plexus has been found in cephalopods. It is possible that the ISF is continuously produced over the whole of the exchange surface (vessel wall) in *Sepia* brain, analogous to the proposed production of brain ISF by the cerebral capillaries in vertebrates (e.g. Bradbury, 1975; Cserr, 1981). The outflow pathway for the hypothesized bulk flow is also not known, but could be equivalent to the system of 'lymphatic channels' observed by Stephens & Young (1969) in *Octopus* brains when the arteries were injected with ink under high pressure.

The finding of an apparent flow of ISF out of brain in an animal group without a choroid plexus/CSF/cerebral ventricular system supports the idea that ISF drainage pathways may exist quite independently of CSF. Moreover, the *Sepia* findings suggest strongly that flowing ISF may be a universal feature of nervous tissue protected by a blood–brain barrier, with important implications for the dynamics and homeostasis of the brain fluid environment not only in vertebrates, but also in invertebrates such as insects, which have a well developed blood–brain barrier.

In contrast to brain, ISF flow does not appear to contribute significantly to tracer loss from muscle.

Significance of the Sepia blood–brain barrier

We conclude that an effective blood–brain barrier is present in *Sepia*, the first clear evidence for such a barrier in any molluscan species. The fact that a barrier is present in cephalopods but not in lower molluscs suggests that a barrier is an advanced evolutionary feature. The presence of barriers in widely separated phyla (chordata, mollusca, arthropoda) further suggests that a barrier has developed several times in evolution.

Sepia is a marine species, with a blood composition well controlled and similar to

sea water; axons and stellate ganglion synapses continue to function in a saline solution based on sea water. Hence the cephalopod barrier is unlikely to be present simply for gross ionic homoeostasis of the neuronal environment, as has been suggested for some insects (Treherne & Pichon, 1972). Rather, the fact that a blood–brain barrier is restricted to species with highly developed central neural functions (such as visual pattern discrimination, precise motor co-ordination, learning, social interactions), suggests that it is protection of *complex integration* of neural activity that is the major function of the barrier in both invertebrates and vertebrates.

Study of the blood–brain interface in *Sepia* has thus shown that invertebrates can develop a blood–brain barrier approaching that of mammals in tightness. The presence of a barrier in *Sepia* suggests that gross ionic homoeostasis (maintaining a neuronal environment different from that of plasma) is not the primary reason for development of a barrier. Instead, the *Sepia* study suggests that a barrier is associated with development of higher integrative function of the central nervous system. Furthermore, evidence for flow of ISF in *Sepia* brain suggests that bulk turnover of ISF may be fundamental to the control of the neuronal micro-environment in all nervous systems with a blood–brain barrier.

We thank Dr Clifford S. Patlak for assistance with the mathematical modelling and for a critical review of the manuscript and the Director of the Marine Biological Association Laboratory, Plymouth, for research facilities. Financial support was provided by the Wellcome Trust, the Nuffield Foundation, The Royal Society (Marshall-Orr Bequest), the Danish Natural Science Research Council (M.B.) and the National Science Foundation, USA (Grant No. BNS 79-24064 to H.F.C.).

REFERENCES

ABBOTT, N. J. & BUNDGAARD, M. (1985). Vascularity and microvessel surface area density in brain and muscle of the cephalopod *Sepia officinalis*. *Journal of Physiology* **365**, 98*P*.

ABBOTT, N. J., BUNDGAARD, M. & CSERR, H. F. (1982). Experimental study of the blood–brain barrier in the cuttlefish, *Sepia officinalis* L. *Journal of Physiology* **326**, 43–44*P*.

ABBOTT, N. J., BUNDGAARD, M. & CSERR, H. F. (1985). Brain vascular volume, electrolytes and blood–brain interface in the cuttlefish, *Sepia officinalis* (Cephalopoda). *Journal of Physiology* **368**, 197–212.

AMTORP, O. (1980). Estimation of capillary permeability of inulin, sucrose and mannitol in rat brain cortex. *Acta physiologica scandinavica* **110**, 337–342.

ASHHURST, D. E. & COSTIN, N. M. (1971). Insect mucosubstances. II. The mucosubstances of the central nervous system. *Histochemical Journal* **3**, 297–310.

BRADBURY, M. W. B. (1975). Ontogeny of mammalian brain–barrier systems. In *Fluid Environment of the Brain*, ed. CSERR, H. F., FENSTERMACHER, J. D. & FENCL, V., pp. 81–103. New York: Academic Press.

BRADBURY, M. (1979). *The Concept of a Blood–Brain Barrier*. Chichester: John Wiley.

BRADBURY, M. W. B., CSERR, H. F. & WESTROP, R. J. (1981). Drainage of cerebral interstitial fluid into deep cervical lymph of the rabbit. *American Journal of Physiology* **240**, F329–336.

BUNDGAARD, M. & CSERR, H. F. (1981). Impermeability of hagfish cerebral capillaries to radiolabelled polyethylene glycols and to microperoxidase. *Brain Research* **206**, 71–81.

COMPER, W. D. & LAURENT, T. C. (1978). Physiological function of connective tissue polysaccharides. *Physiological Reviews* **58**, 255–315.

CSERR, H. F. (1971). Physiology of the choroid plexus. *Physiological Reviews*. **51**, 273–311.

CSERR, H. F. (1981). Convection of brain interstitial fluid. In *Advances in Physiological Science*, vol. 7, *Cardiovascular Physiology, Microcirculation and Capillary Exchange*, ed. KOVACH, A. G. B., HAMAR, J. & SZABO, L., pp. 337–341. Budapest: Pergamon Press.

CSERR, H. F., COOPER, D. N. & MILHORAT, T. H. (1977). Flow of cerebral interstitial fluid as

indicated by the removal of extracellular markers from rat caudate nucleus. In *The Ocular and Cerebrospinal Fluids*, ed. BITO, L. Z., DAVSON, H. & FENSTERMACHER, J. D., pp. 461–473. London: Academic Press.

CSERR, H. F., COOPER, D. N., SURI, P. K. & PATLAK, C. S. (1981). Efflux of radiolabeled polyethylene glycols and albumin from rat brain. *American Journal of Physiology* **240**, F319–328.

CSERR, H. F. & OSTRACH, L. H. (1974). Bulk flow of interstitial fluid after intracranial injection of Blue Dextran 2000. *Experimental Neurology* **45**, 50–60.

DAVSON, H., KLEEMAN, C. F. & LEVIN, E. (1963). The blood–brain barrier. In *Drugs and Membranes*, ed. HOGBEN, A. M. & LINDGREN, P., pp. 71–94. Oxford: Pergamon Press.

FENSTERMACHER, J. D., BLASBERG, R. G. & PATLAK, C. S. (1981). Methods for quantifying the transport of drugs across brain barrier systems. *Pharmacology and Therapeutics* **14**, 217–248.

MARGOLIS, R. U. & MARGOLIS, R. K. (ed.). (1979). *Complex Carbohydrates of Nervous Tissue*. New York: Plenum.

NICHOLSON, C. & PHILLIPS, J. M. (1981). Ion diffusion modified by tortuosity and volume fraction in the extracellular microenvironment of the rat cerebellum. *Journal of Physiology* **321**, 225–257.

OHNO, K., PETTIGREW, K. D. & RAPOPORT, S. I. (1978). Lower limits of cerebrovascular permeability to non-electrolytes in the conscious rat. *American Journal of Physiology* **235**, H299–307.

PAASKE, W. P. (1980). Permeability of capillaries in muscle, skin, and subcutaneous tissue. *The Physiologist* **23**, 75–78.

POOLE-WILSON, P. A. & CAMERON, I. R. (1975). ECS, intracellular pH, and electrolytes of cardiac and skeletal muscle. *American Journal of Physiology* **229**, 1299–1304.

ROSENBERG, G. A., KYNER, W. T. & ESTRADA, E. (1980). Bulk flow of brain interstitial fluid under normal and hyperosmolar conditions. *American Journal of Physiology* **238**, F42–49.

SCHMIDT-NIELSEN, B. & RENFRO, J. L. (1975). Kidney function of the American eel *Anguilla rostrata*. *American Journal of Physiology* **228**, 420–431.

SCHMIDT-NIELSEN, B., RENFRO, J. L. & BENOS, D. (1972). Estimation of extracellular space and intracellular ion concentrations in osmoconformers, hypo- and hyperosmoregulators. *The Bulletin of the Mount Desert Island Biological Laboratory* **12**, 99–104.

STEPHENS, P. R. & YOUNG, J. Z. (1969). The glio-vascular system of cephalopods. *Philosophical Transactions of the Royal Society B* **255**, 1–11.

SZENTISTVANYI, I., PATLAK, C. S., ELLIS, R. A. & CSERR, H. F. (1984). Drainage of interstitial fluid from different regions of rat brain. *American Journal of Physiology* **246**, F835–844.

TREHERNE, J. E. & PICHON, Y. (1972). The insect blood–brain barrier. *Advances in Insect Physiology* **9**, 257–313.

WEIBEL, E. R. (1979). *Stereological Methods*, vol. 1., p. 93. London: Academic Press.